Colloids and Surfaces B: Biointerfaces 84 (2011) 97–102

Contents lists available at ScienceDirect

Colloids and Surfaces B: Biointerfaces

journal homepage: www.elsevier.com/locate/colsurfb

# Preparation and characterization of electrospun PLGA/gelatin nanofibers as a potential drug delivery system

Z.X. Meng[a], X.X. Xu[a], W. Zheng[a], H.M. Zhou[a], L. Li[a], Y.F. Zheng[a,b,*], X. Lou[a,c]

[a] Center for Biomedical Materials and Engineering, Harbin Engineering University, Harbin 150001, China
[b] Department of Advanced Materials and Nanotechnology, College of Engineering, Peking University, Beijing 100871, China
[c] Department of Chemical Engineering, Curtin University of Technology, Kent Street, Bentley, WA 9102, Australia

ARTICLE INFO

*Article history:*
Received 16 July 2010
Received in revised form
11 December 2010
Accepted 14 December 2010
Available online 21 December 2010

*Keywords:*
Electrospinning
PLGA
Gelatin
Scaffold
Drug delivery

ABSTRACT

Drug (Fenbufen, FBF)-loaded poly(D,L-lactide-co-glycolide) (PLGA) and PLGA/gelatin nanofibrous scaffolds were fabricated via electrospinning technique. The influences of gelatin content, fiber arrangement, crosslinking time and pH value of the buffer solution on FBF release behavior of the resulting nanofibrous scaffolds were investigated, with the corresponding FBF-loaded PLGA and PLGA/gelatin solvent-cast films as controls. The release rate of FBF was found to be increased with the increment of gelatin content for all the composite samples, and the FBF release rate of aligned nanofibrous scaffold was lower than that of randomly oriented scaffold. Moreover, the crosslinking treatment depressed effectively the burst release of FBF at initial release stage of PLGA/gelatin (9/1) nanofibrous scaffold. In addition, the pH value of the buffer solution could change the physical state of the polymer and affect the FBF release rate.



## 1. Introduction

Medication plays an important role in the medical treatment. Most of the drugs would take their curative effect only when their concentrations in the blood are above their minimum effective level. However, each kind of drug has its own biological half-life and cannot maintain an effective concentration for a long time. Merely increasing the dose of drug will extend itself into the toxic response region, whereas taking the selected dose of drug for several times during a period of time (e.g. three times a day) is not convenient for the patient. In this case, drug controlled release formulations and devices exhibit particular advantage because they can maintain the desired drug concentration in blood for a long period of time without reaching a toxic level or dropping below the minimum effective level. The drug controlled release system such as micelle, hydrogel and microparticle has been described in recent publications [1–12]. For example, pH-sensitive micelle or hydrogel showed higher pH-responsiveness at the focus than free drug, which significantly increased therapeutic efficacy with minimum side effects by other tissues [4,5]. However, these drug controlled release systems always need complicated modification such as surface modification, which would affect the drug activity.

During the past few years, the fabrication of polymer-based nanofibers by electrospinning has attracted considerable attention in biomedical fields. Under the critical electric field, the ultrafine jet would eject from charged polymer fluid and then change themselves into nanofibers with the rapid evaporation of the solvent. The prominent advantages of three-dimensional electrospun nanofibrous scaffolds such as high surface area, high porosity and controllable pore size have made them widely used as tissue engineering scaffolds [13–18], wound dressing articles [19–22] and drug carriers [23–26].

As a drug carrier, the electrospun nanofibers possess high surface-to-volume ratio which would accelerate the solubility of drug in the aqueous solution and enhance the efficiency of the drug. Furthermore, many parameters, such as solution properties, voltage, and collector distance between the spinneret and the collecting plate, along with external factors like temperature and humidity, etc., would influence the structure and surface morphologies of nanofibers, which can control the release rate and amount of the drug [27]. On the other hand, biodegradable polymer as drug carrier would protect drug from the corrosion of gastric acid and enzyme, which can preserve the activity of the drug. For example, the core–shell structured electrospun fibers protected the structural integrity of encapsulated protein during incubation in the medium [28]. Otherwise, the electrospun nanofiber can also be used as template to produce conducting drug-loaded polymer nan-

* Corresponding author at: Department of Advanced Materials and Nanotechnology, College of Engineering, Peking University, Beijing 100871, China. Tel.: +86 10 6276 7411; fax: +86 10 6276 7411.
*E-mail address:* yfzheng@pku.edu.cn (Y.F. Zheng).

0927-7765/$ – see front matter © 2010 Elsevier B.V. All rights reserved.
doi:10.1016/j.colsurfb.2010.12.022

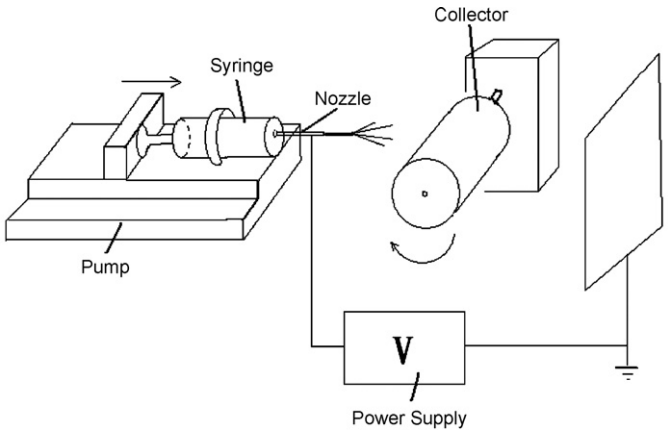


**Fig. 1.** Schematic of electrospinning apparatus used in the process of making PLGA and PLGA/gelatin nanofibrous scaffolds.

otube in order to realize the controlled drug release by electrical stimulation [29].

In this study, we attempt to produce poly(D,L-lactide-co-glycolide)/gelatin composite nanofibrous scaffold as a drug carrier with the combined advantages of the suitable mechanical property, the bioactive surface and controllable degradability. Fenbufen (FBF), a non-steroidal anti-inflammatory drug commonly used for the relief of symptoms of rheumatoid arthritis and osteoarthritis [30] was loaded into PLGA/gelatin nanofibers during the electrospinning process. The morphology of drug loaded nanofiber, the swelling behavior in the aqueous medium, and the actual FBF release characteristics were investigated systematically, using the corresponding solvent-cast polymer films as controls.

## 2. Materials and methods

### 2.1. Materials

Poly(D,L-lactide-co-glycolide) (LA/GA 85/15, $M_w$ = 200,000) was purchased from Jinan Daigang Biomaterial Co. Ltd. (China). Gelatin was purchased from Tianjin Bodi Chemical Co. Ltd. (China). 2,2,2-Trifluoroethanol (TFE) was selected as the solvent and was purchased from Aladdin Regent Co. Ltd. (China). Fenbufen was obtained from Group Sanjing Pharmaceutical Co. Ltd. (China). All chemicals were used directly without further purification. All solutions were prepared using doubly distilled water.

### 2.2. Preparation of FBF-loaded electrospun scaffolds and films

The experimental polymer composite solutions were prepared by dissolving PLGA and gelatin with a weight ratio of 10:0, 9:1 in 2,2,2-trifluoroethanol. Subsequently, FBF was added into the composite solution with the concentration of 2 mg/mL and the mixture was stirred for 12 h at room temperature to ensure a complete dissolution of the drug and eventually obtained homogeneous composite solutions for electrospinning.

The apparatus of electrospinning in this work is shown in Fig. 1. For electrospinning, 5 mL of the composite solution was placed in a 5 mL syringe fitted with a stainless-steel blunt needle of 0.5 mm in diameter and an injection rate of 0.5 mL/h using an infusion pump (TS2-60, Baoding Longer Precision Pump Co. Ltd., China). The needle tip of the syringe was connected with the high voltage power supply (HB-F303-1-AC, China) with the applied voltage of 10 kV. Randomly oriented nanofibers were simply collected by a flat collector wrapped with aluminum foil which was kept at a distance of 10 cm from the needle tip. Aligned nanofibers were collected using a rotating drum with 50 mm diameter at a rotation speed of 3000 rpm. The resulting electrospun nanofibers with FBF loading were further crosslinked in glutaraldehyde vapor for varying period of time. For the comparison purpose, corresponding solvent-cast film samples were also prepared [31]. All samples were dried overnight under vacuum at room temperature.

### 2.3. Characterizations of FBF-loaded electrospun scaffolds and films

The morphologies of FBF-loaded electrospun nanofibrous scaffolds were examined by a scanning electron microscope (SEM) (CamScan MX2600FE, UK) at an accelerating voltage of 20 kV. The electrospun nanofibrous scaffold samples were coated with a thin layer of platinum in double 30 s consecutive cycles at 45 mA to reduce charging and produce conductive surfaces. The diameters of nanofibers were analyzed using software Image J.

To evaluate the swelling behavior which could originate at the physiological condition, the FBF-loaded electrospun nanofibrous scaffolds as well as FBF-loaded solvent-cast films with known weights (denoted as $m_d$) were put in test tubes containing 10 mL phosphate buffer solutions (pH 7.4) each and incubated for 24 h at 37 °C. Then the water on the specimen surfaces were removed with filter paper and the specimens were weighed in wet condition (denoted as $m_w$). The swelling ratio was calculated according to the following equation for each sample [32]:

$$\text{Swelling ratio } (\%) = \frac{m_w - m_d}{m_d} \times 100\% \quad (1)$$

The thermal properties of FBF powder and FBF-loaded electrospun nanofibrous scaffolds were investigated by the differential scanning calorimetry (DSC) measurements (Perkin–Elmer Company, USA) in the temperature range from −50 °C to 300 °C at a heating rate of 15 °C/min under a nitrogen atmosphere. For thermogravimetric analysis (TGA), the samples were heated up to 600 °C at a constant heating rate of 10 °C/min, under a constant nitrogen flow rate of 50 mL/min through the sample chamber.

### 2.4. Actual drug content

The drug-loaded sample was dissolved in 5 mL TFE and the actual amount of FBF was measured using a UV-Vis spectrometer at λ = 280 nm (Shimadzu UV-2550, Japan). Then the actual drug amount contained in the sample was back calculated from the obtained data against a predetermined calibration curve of drugs. The calibration curve of FBF was carried out in the concentration ranging from 0.002 mg/mL to 0.02 mg/mL.

### 2.5. Drug release

The drug-loaded sample was incubated at 37 °C in 10 mL of phosphate buffer solution (pH 7.4). At certain incubation time points, the sample was transferred into 10 mL of fresh buffer solution. The released FBF in the buffer solution was determined by a UV-Vis spectrophotometer at the same wavelength.

### 2.6. Statistical analysis

A software of origin 7.0 (Origin Lab Inc., USA) was used to analyze the obtained data. Values ($n$ = 3) were averaged and expressed as means ± standard deviation (SD).

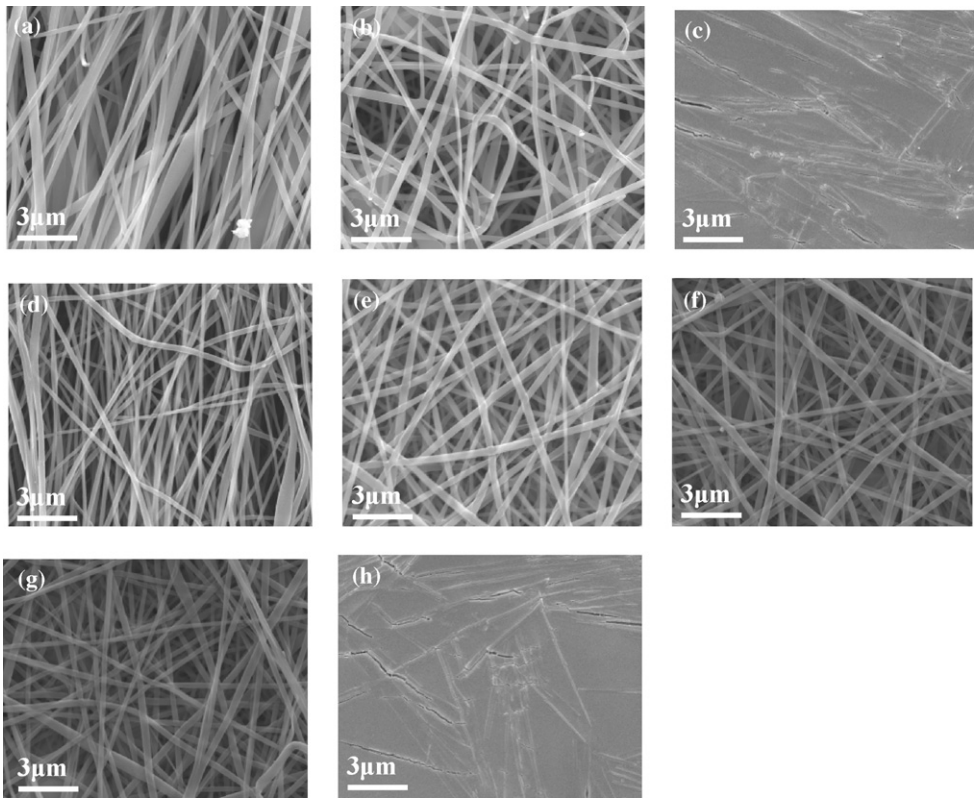


**Fig. 2.** SEM image showing the morphology of electrospun FBF-loaded PLGA nanofibers (a, b) and corresponding solvent-cast film (c); FBF-loaded PLGA/gelatin (9/1) nanofibers (d–g) and corresponding film (h); aligned nanofibers (a, d); crosslinked by glutaraldehyde vapor for 2 h (f) and 5 h (g).

## 3. Results and discussion

### 3.1. Morphology observation

Fig. 2 shows the SEM images of FBF-loaded electrospun nanofibrous scaffolds and solvent-cast films. It can be seen that the randomly oriented FBF-loaded PLGA and PLGA/gelatin (9/1) nanofibers possessed smooth surface with the average fiber diameters of $342 \pm 34$ nm and $313 \pm 69$ nm, respectively, whereas the average fiber diameters of the aligned FBF-loaded PLGA and PLGA/gelatin (9/1) nanofibers were $335 \pm 52$ nm and $310 \pm 24$ nm, respectively. It showed that the diameter of the resulting nanofibers decreased with the addition of gelatin. A possible reason is that the addition of gelatin increased the charge density of the solution which improved the stretching force and the self-repulsion of the jet, and thus decreased the fiber diameter [33,34]. There was no drug aggregates on the surface of the FBF-loaded nanofibers. However, it was obvious that the drug crystal appeared on the surface of the solvent-cast films, which due to the evaporation of solvent from the film was much slower than that from the electrospinning process [35]. In addition, the previous works showed that the crosslinked gelatin could decrease the drug release in aqueous solution [36,22]. Thus the FBF-loaded PLGA/gelatin nanofibrous scaffold was further crosslinked in glutaraldehyde vapor for different period of time, in order to investigate the influence of crosslinking on drug release character in this study. From Fig. 2e–g, it seemed that there was no significant difference on the morphology of PLGA/gelatin (9/1) nanofibers before and after crosslinking.

### 3.2. Swelling ratio

The FBF-loaded electrospun nanofibrous scaffolds and solvent-cast films were characterized to determine the swelling behavior through incubating samples in the phosphate buffer solution (pH 7.4) at 37 °C for 24 h. As can be seen from Table 1, the swelling ratio of randomly oriented PLGA nanofibrous scaffolds was $152 \pm 18\%$ and the PLGA/gelatin (9/1) nanofibrous scaffold was $376 \pm 28\%$, demonstrating a significantly improved hydrophilicity of the composite nanofibers. The swelling ratios of aligned PLGA and PLGA/gelatin (9/1) nanofibrous scaffolds were $137 \pm 11\%$ and $318 \pm 30\%$, which were lower than those of corresponding randomly oriented ones. The swelling ratio of randomly oriented PLGA/gelatin (9/1) nanofibrous scaffold was reduced after crosslinking, which was consistent to the previous reports [32,33]. In comparison with the solvent-cast films ($5 \pm 2\%$ for PLGA film and $23 \pm 11\%$ for PLGA/gelatin (9/1) film), all the FBF-loaded nanofibrous scaffolds including the randomly oriented and the well-aligned with/without crosslinking treatment showed higher swelling ratio. This could be possibly due to the large amount of water retained in the interconnected fibrous pores by the capillary action [37].

### 3.3. Thermal properties

The thermal properties of FBF powder and various FBF-loaded electrospun nanofibrous scaffolds were characterized using DSC and TGA. Fig. 3A shows DSC thermograms for the FBF powder, FBF-loaded electrospun PLGA, PLGA/gelatin (9/1) nanofibrous scaffolds, respectively. A single sharp endothermic curve with the peak temperature of 188 °C was seen on the DSC thermogram of pure FBF powder, corresponding to the melting transition of the FBF [38]. However, no peak presented on the DSC thermograms of FBF-loaded electrospun nanofibrous scaffold, indicating that FBF was in amorphous phase condition within the FBF-loaded electrospun nanofibers [31]. This might be due to the rapid evaporation of the solvent during the electrospinning process which hindered the for-

**Table 1**
Swelling ratio of FBF-loaded PLGA and PLGA/gelatin nanofibrous scaffolds (%).

| Sample of PLGA/gelatin | Aligned nanofiber | Randomly oriented nanofiber | Randomly oriented nanofiber crosslinking for 2 h | Randomly oriented nanofiber crosslinking for 5 h | Solvent-cast film |
|---|---|---|---|---|---|
| 10/0 | 137 ± 11 | 152 ± 19 | – | – | 5 ± 2 |
| 9/1 | 318 ± 30 | 376 ± 29 | 271 ± 46 | 173 ± 19 | 23 ± 11 |

mation of the FBF crystal. It may also be caused by the limited amount of FBF contained in the nanofibers.

Fig. 3B presents the comparative thermogravimetric curves of FBF powder, FBF-loaded PLGA and PLGA/gelatin (9/1) nanofibrous scaffolds. It was found that after the large weight loss, there remained char content of about 2% for the case of FBF-loaded PLGA nanofibers and about 11% for the FBF-loaded PLGA/gelatin (9/1) composite fibers at around 370 °C, which was very close to the weight of drug and gelatin content (2 wt.% + 10 wt.%), and demonstrated that the large weight loss was almost the decomposition of PLGA. When the temperature arrived at 600 °C, there was still some char content existing in the case of FBF powder but no char content left in the case of FBF-loaded PLGA nanofiber and FBF-loaded PLGA/gelatin nanofiber (9/1) scaffolds. This might be due to the different physical state of FBF in the FBF-loaded nanofibers and FBF powder, and FBF in amorphous phase within the nanofibers was less stable than FBF powder.

### 3.4. Drug release

The actual amount of FBF in the FBF-loaded electrospun nanofibrous scaffolds and corresponding solvent-cast films were determined, as listed in Table 2. It can be seen that the actual amount of FBF in the electrospun nanofibrous scaffolds and the film counterparts were higher than 97% (based on the weight of drug used in the solutions). The values were used as basis to calculate the drug release from the drug-loaded samples. Fig. 4A shows the release profiles of FBF from the FBF-loaded randomly oriented PLGA and PLGA/gelatin (9/1) nanofibrous scaffolds and their corresponding films. At 1500 min, the release amount of drug from the PLGA scaffold was about 47%. The drug released from the PLGA/gelatin (9/1) nanofibrous scaffolds increased significantly with the addition of gelatin content. It was almost 100% for the composite scaffold after 1500 min. A burst release was observed from the release profile of FBF-loaded PLGA/gelatin (9/1) nanofibrous scaffold. Due to

**Table 2**
Actual amount of FBF in the FBF-loaded electrospun nanofibers and corresponding solvent-cast films.

| Sample of PLGA/gelatin | Actual amount of FBF based on the initial amount of FBF loaded (%) | |
|---|---|---|
| | FBF-loaded electrospun nanofibers | FBF-loaded solvent-cast films |
| 10/0 | 99.13 ± 3.54 | 98.45 ± 2.32 |
| 9/1 | 97.89 ± 5.98 | 97.64 ± 7.31 |

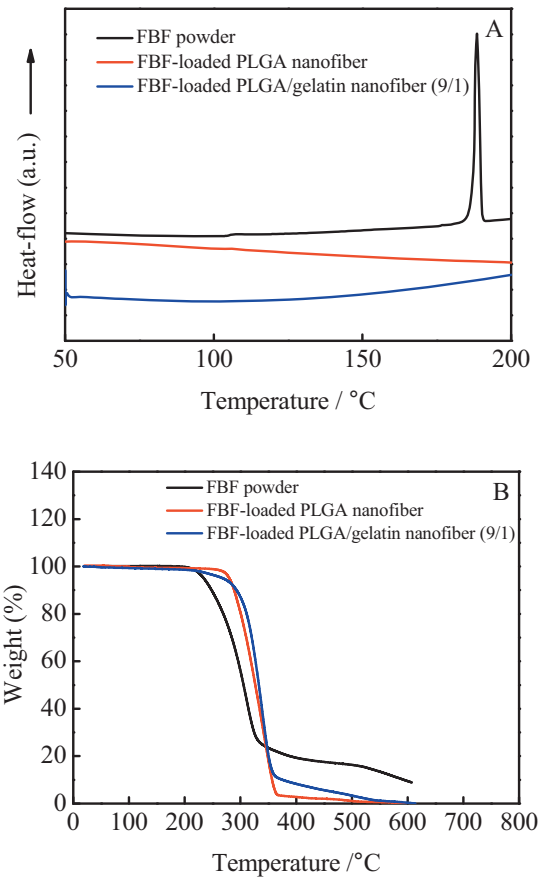


**Fig. 3.** Thermal properties of FBF powder, FBF-loaded PLGA and PLGA/gelatin electrospun nanofibers, (A) DSC and (B) TGA.

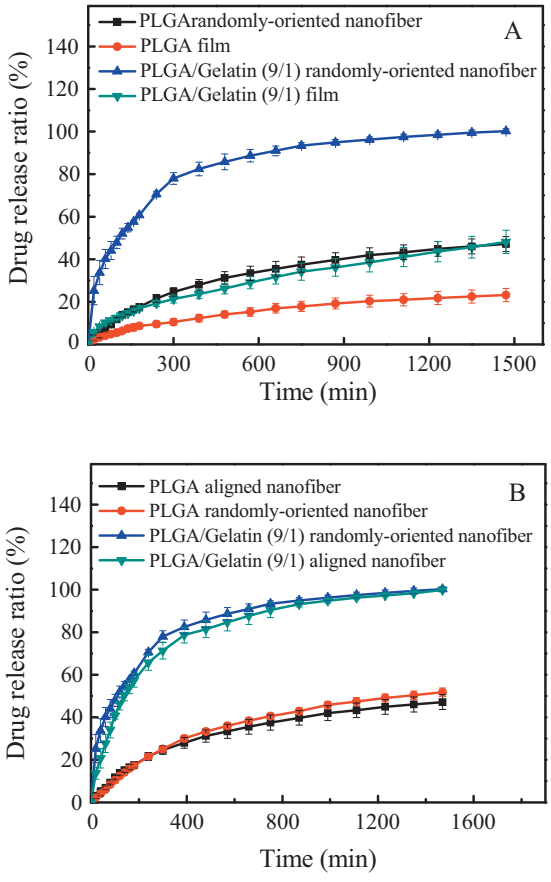


**Fig. 4.** Release curves of FBF from FBF-loaded PLGA and PLGA/gelatin (9/1) electrospun nanofibers and solvent-cast films (A), aligned and randomly oriented PLGA and PLGA/gelatin (9/1) electrospun nanofibers (B).

the diffusion-controlled release of the drug and the higher water adsorption of the scaffold, therefore the drug molecule had a more rapid diffusion from the matrix into the aqueous medium [39]. In comparison with the electrospun PLGA/gelatin (9/1) composite nanofibrous scaffold, the corresponding FBF-loaded solvent-cast film showed a much slower drug release rate (Fig. 4A). Some acicular drug crystals appeared on the surface of the FBF-loaded solvent-cast films, as shown in Fig. 2c and h, which demonstrated that the FBF release pattern of the film was different from that of electrospun nanofiber. It might be explained by the drug crystal dissolution associated with the drug diffusion within the films [35]. Moreover, the electrospun nanofibrous scaffolds possessed the higher surface area and higher swelling ratio than those of solvent-cast films, allowing more drug molecules to diffuse from the nanofibers to the surrounding medium. Therefore, the drug release rate and the maximum amount of the drug released from the FBF-loaded films were much lower than that of the electrospun nanofibrous scaffolds.

The influence of nanofiber orientation on drug release characteristic was further investigated. Fig. 4B shows the release characteristics of FBF from the aligned and randomly oriented FBF-loaded electrospun PLGA and PLGA/gelatin (9/1) nanofibrous scaffolds. As can be seen, the drug release behavior from aligned nanofibrous scaffolds was similar to that of the randomly oriented nanofibrous scaffolds, but the drug release rate from the aligned nanofibrous scaffold was much slower. It was known that the parallel well-aligned nanofibers often contained decreased porosity in comparison with the randomly oriented nanofibrous scaffold, which could be proved by the lower swelling ratio (see Table 1). Thus the drug diffusing outwards from the aligned scaffold was much difficult than that from randomly oriented scaffold.

Fig. 5 shows the FBF release behavior of FBF-loaded PLGA/gelatin (9/1) nanofibrous scaffolds with different crosslinking time. As shown in Fig. 5, the pattern of FBF release curve did not change with the increase of crosslinking time. However, the release rate and the maximum amount of FBF released from FBF-loaded electrospun nanofibrous scaffold decreased with the increasing of crosslinking time, which might attribute to the fact that the enhanced intermolecular force by crosslinking inhibited the diffusion of drug, and resulted in slowing-down the drug release rate [36]. Moreover, with the increasing of crosslinking time, the release of FBF-loaded PLGA/gelatin (9/1) nanofibrous scaffold generally approached to a uniform value, which demonstrated that crosslinking treatment would control the burst release of drug effectively.

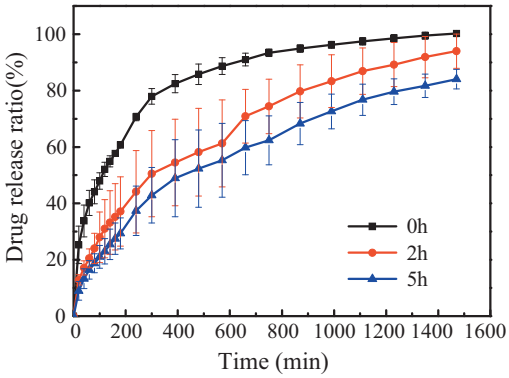


**Fig. 5.** Release curves of FBF from PLGA/gelatin (9/1) electrospun nanofibers with different crosslinking time (0, 2, 5 h).

Fig. 6 depicts the FBF release behavior of FBF-loaded electrospun PLGA and PLGA/gelatin (9/1) nanofibrous scaffolds, with corresponding solvent-cast films as comparison. The FBF release curve patterns of various nanofibrous scaffolds and solvent-cast films were obviously similar in medium with different pH values, but the release rate of FBF increased with increasing pH value from 5 to 9. These results were consistent to the results reported by Faisant et al., who found that the glass transition temperature of

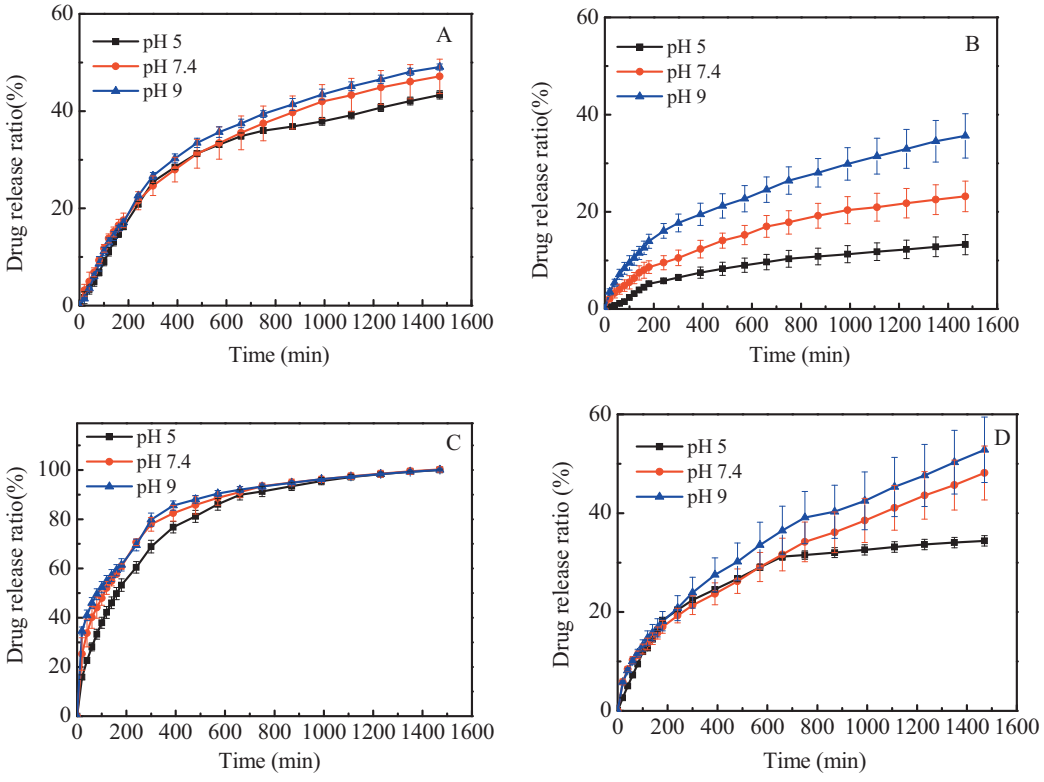


**Fig. 6.** Release curves of FBF from PLGA/gelatin electrospun nanofibers (A, C) and solvent-cast films (B, D) with different pH values.

the matrix polymer was changed in mediums with different pH values (above 37 °C at pH 1.3 and 4.5; below 37 °C at pH 7.4 and 10.8), exhibiting different physical states of matrix polymer [40]. The mobility of polymer chains would increase when the physical state of polymer changed from glassy state to rubbery state, which would accelerate the diffusion of the drug. Furthermore, the acidic molecule FBF is more soluble in the alkaline medium, leading to increasing drug release with the pH value of medium increasing. On the other hand, it was obvious that the difference of drug release rate among solvent-cast films under different pH values was larger than that in the form of nanofibrous scaffolds. This may be because the drug release pattern for film samples was the dissolution of drug crystal associating with the drug diffusion, and increasing pH value of medium would enhance the dissolution of drug crystal. Clearly as drug carrier, the nanofibrous scaffold was more stable than solvent-cast film in the medium with different pH values.

## 4. Conclusions

In this study, FBF-loaded electrospun PLGA and PLGA/gelatin (9/1) nanofibrous scaffolds as well as FBF-loaded solvent-cast films were produced and their drug release characteristics were further investigated. Smooth surface morphology was found for all nanofibers whereas drug aggregates appeared on the surface of FBF-loaded films. Increased gelatin contents enhanced the hydrophilicity of PLGA/gelatin scaffolds leading to the increase of FBF release rate. Meanwhile the nanofiber orientation could influence the FBF release pattern from the FBF-loaded PLGA/gelatin nanofibrous scaffolds. The crosslinking treatment with glutaraldehyde vapor resulted in the reduced drug release rate. The pH value of buffer solution could change the physical state of polymer matrix which affected the release rate of the drug, and the nanofibrous scaffold was more stable in buffer solution with different pH value compared with the solvent-cast films.

## Acknowledgements

This work is supported by the Research Fund for the Doctoral Program of Higher Education under Grant (No. 20060217012) and the Fundamental Research Funds for the Central Universities (No. HEUCF101021).

## References

[1] C. Civiale, M. Licciardi, G. Cavallaro, G. Giammona, M.G. Mazzone, Int. J. Pharm. 378 (2009) 177–186.
[2] J. Guan, N. Ferrell, L.J. Lee, D.J. Hansford, Biomaterials 27 (2006) 4034–4041.
[3] M. Hirose, A. Tachibana, T. Tanabe, Mater. Sci. Eng. C 30 (2010) 664–696.
[4] K.H. Min, J.-H. Kim, S.M. Bae, H. Shin, M.S. Kim, S. Park, H. Lee, R.-W. Park, I.-S. Kim, K. Kim, I.C. Kwon, S.Y. Jeong, D.S. Lee, J. Control. Release 144 (2010) 259–266.
[5] I. Colinet, V. Dulong, G. Mocanu, L. Picton, D. Le Cerf, Eur. J. Pharm. Biopharm. 73 (2009) 345–350.
[6] J. Wu, W. Wei, L.-Y. Wang, Z.-G. Su, G.-H. Ma, Colloids Surf. B 63 (2008) 164–175.
[7] G.A. Husseini, G.D. Myrup, W.G. Pitt, D.A. Christensen, N.Y. Rapoport, J. Control. Release 69 (2000) 43–52.
[8] K.T. Oh, Y.T. Oh, N.-M. Oh, K. Kim, D.H. Lee, E.S. Lee, Int. J. Pharm. 375 (2009) 163–169.
[9] F. Brandl, F. Kastner, R.M. Gschwind, T. Blunk, J. Teßmar, A. Göpferich, J. Control. Release 142 (2010) 221–228.
[10] B. Jeong, Y.H. Bae, S.W. Kim, J. Control. Release 63 (2000) 155–163.
[11] R. Jeyanthi, K.P. Rao, J. Control. Release 13 (1990) 91–98.
[12] X.J. Loh, P. Peh, S. Liao, C. Sng, J. Li, J. Control. Release 143 (2010) 175–182.
[13] M. Li, Y. Guo, Y. Wei, A.G. MacDiarmid, P.I. Lelkes, Biomaterials 27 (2006) 2705–2715.
[14] F. Yang, R. Murugan, S. Wang, S. Ramakrishna, Biomaterials 26 (2005) 2603–2610.
[15] J. Lannutti, D. Reneker, T. Ma, D. Tomasko, D. Farson, Mater. Sci. Eng. C 27 (2007) 504–509.
[16] Z.X. Meng, Y.S. Wang, C. Ma, W. Zheng, L. Li, Y.F. Zheng, Mater. Sci. Eng. C 30 (2010) 1204–1210.
[17] T.A. Telemeco, C. Ayres, G.L. Bowlin, G.E. Wnek, E.D. Boland, N. Cohen, C.M. Baumgarten, J. Mathews, D.G. Simpson, Acta Biomater. 1 (2005) 377–385.
[18] L. Buttafoco, N.G. Kolkman, P. Engbers-Buijtenhuijs, A.A. Poot, P.J. Dijkstra, I. Vermes, J. Feijen, Biomaterials 27 (2006) 724–734.
[19] M. Ignatova, N. Manolova, I. Rashkov, Eur. Polym. J. 43 (2007) 1609–1623.
[20] J.-P. Chen, G.-Y. Chang, J.-K. Chen, Colloids Surf. A 313–314 (2008) 183–188.
[21] K.S. Rho, L. Jeong, G. Lee, B.-M. Seo, Y.J. Park, S.-D. Hong, S. Roh, J.J. Cho, W.H. Park, B.-M. Min, Biomaterials 27 (2006) 1452–1461.
[22] P. Rujitanaroj, N. Pimpha, P. Supaphol, Polymer 49 (2008) 4723–4732.
[23] S.K. Tiwari, R. Tzezana, E. Zussman, S.S. Venkatraman, Int. J. Pharm. 392 (2010) 209–217.
[24] E. Kenawy, F.I. Abdel-Hay, M.H. El-Newehy, G.E. Wnek, Mater. Chem. Phys. 113 (2009) 296–302.
[25] Y. Su, X. Li, S. Liu, X. Mo, S. Ramakrishna, Colloids Surf. B 73 (2009) 376–381.
[26] X. Li, Y. Su, S. Liu, L. Tan, X. Mo, S. Ramakrishna, Colloids Surf. B 75 (2010) 418–424.
[27] S. Chakraborty, I.-C. Liao, A. Adler, K.W. Leong, Adv. Drug Deliv. Rev. 61 (2009) 1043–1054.
[28] Y. Yang, X. Li, W. Cui, S. Zhou, R. Tan, C. Wang, J. Biomed. Mater. Res. A 86A (2008) 374–385.
[29] M.R. Abidian, D.-H. Kim, D.C. Martin, Adv. Mater. 18 (2006) 405–409.
[30] G. Carlucci, P. Mazzeo, G. Palumbo, J. Chromatogr. B 682 (1996) 315–319.
[31] O. Suwantong, P. Opanasopit, U. Ruktanonchai, P. Supaphol, Polymer 48 (2007) 7546–7557.
[32] S.-Y. Gu, Z.-M. Wang, J. Ren, C.-Y. Zhang, Mater. Sci. Eng. C 29 (2009) 1822–1828.
[33] L. Ghasemi-Mobarakeh, M.P. Prabhakaran, M. Morshed, M. Nasr-Esfahani, S. Ramakrishna, Biomaterials 29 (2008) 4532–4539.
[34] J. Lee, G. Tae, Y.H. Kim, I.S. Park, S. Kim, S.H. Kim, Biomaterials 29 (2008) 1872–1879.
[35] S. Tungprapa, I. Jangchud, P. Supaphol, Polymer 48 (2007) 5030–5041.
[36] D. Yang, Y. Li, J. Nie, Carbohydr. Polym. 69 (2007) 538–543.
[37] Y. Jia, J. Gong, X.H. Gu, H. Kim, J. Dong, X. Shen, Carbohydr. Polym. 67 (2007) 403–409.
[38] C.M. Wassvik, A.G. Holmen, C.A.S. Bergstrom, I. Zamora, P. Artursson, Eur. J. Pharm. Sci. 29 (2006) 294–305.
[39] F. Mi, S. Shyu, Y. Lin, Y. Wu, C. Peng, Y. Tsai, Biomaterials 24 (2003) 5023–5036.
[40] N. Faisant, J. Akiki, F. Siepmann, J.P. Benoit, J. Siepmann, Int. J. Pharm. 314 (2006) 189–197.